Eur. Phys. J. A **17**, 375–379 (2003)
DOI 10.1140/epja/i2002-10180-y

THE EUROPEAN PHYSICAL JOURNAL A

Double-spin asymmetries in electron-nucleon scattering in Halls B and C at JLab

D.G. Crabb[a]

Physics Department, University of Virginia, Charlottesville, VA 22903, USA

Received: 1 November 2002 /
Published online: 15 July 2003 – © Società Italiana di Fisica / Springer-Verlag 2003

Abstract. Three experiments at JLab have measured the double polarization asymmetries $A_\parallel(x,Q^2)$ in the nucleon resonance region, using polarized electron beams incident on polarized proton and deuteron targets. The analysis for the first experiment, eg1a in Hall B, is nearly finished and preliminary values of the spin structure function $g_1(x,Q^2)$ and the first moment Γ_1 (x) have been extracted. The other two experiments, one in Hall B and one in Hall C, are still analysing data. Some results are presented.

PACS. 24.70.+s Polarization phenomena in reactions

1 Introduction

In recent years, measurements of the spin-dependent structure functions g_1 and g_2 for the proton and neutron, in the deep inelastic scattering region (DIS) have established that only about 25% of the spin of the nucleon is carried by the quarks. This is in disagreement with quark model predictions. At the same time, the behaviour of the structure functions in the resonance region, where approximations used in DIS may have little validity, has received little attention. The Q^2 evolution of the structure functions from the DIS region to the resonance region is also of great interest and has also been little studied.

At $Q^2 = 0$ a constraint on the moments of the nucleon spin structure functions is provided by the Gerasimov-Drell-Hearn (GDH) sum rule [1]:

$$\int_{\nu_{\rm thresh}}^{\infty} \frac{\sigma_{1/2}(x,Q^2=0)-\sigma_{3/2}(x,Q^2=0)}{\nu}{\rm d}\nu = -\frac{2\pi^2\alpha}{M^2}\kappa_N^2,$$

which relates the difference in the helicity-dependent total photoabsorption cross-sections to the anomalous magnetic moment κ of the target nucleon, where $\nu_{\rm thresh}$ is the photon energy at pion threshold, M is the nucleon mass and α the fine-structure constant. This sum rule has been tested up to 800 MeV at Mainz [2] and up to 2 GeV at Bonn [3] for protons.

Ji and Osbourne [4] have proposed an extension of this sum rule to finite Q^2, which relates the first moment Γ_1 of the structure function to κ^2:

$$\Gamma_1(Q^2 \longrightarrow 0) \Longrightarrow \frac{Q^2}{16\pi^2\alpha}\int_{\nu_{\rm thresh}}^{\infty} \frac{\sigma_{1/2}-\sigma_{3/2}}{\nu}{\rm d}\nu = -\frac{Q^2}{8M^2}\kappa^2.$$

Because Γ_1^p in the DIS region is positive, it must cross to negative values and approach zero with a negative slope as $Q^2 \Longrightarrow 0$.

Measurements of Γ_1 at low Q^2, together with the evolution of DIS measurements down to low Q^2 will allow stringent tests of nucleon structure models.

In this paper, I present some results from three experiments conducted at JLab measuring g_1 for both the proton and neutron and also g_2 in the case of one of the experiments. The experiments were 1) eg1a, a limited statistics and limited kinematic coverage experiment using CLAS in Hall B, 2) eg1b, essentially the same as eg1a, except with a larger kinematic reach and many more events accumulated and 3) RSS in Hall C, where g_2 for the neutron and proton was also measured.

2 Experiments

All three experiments extracted g_1 through measuring the inclusive scattering asymmetry $A_\parallel$ of polarized electrons off polarized nucleons, where $A_\parallel$ is given by

$$A_\parallel = \frac{N^{\uparrow\downarrow} - N^{\uparrow\uparrow}}{N^{\uparrow\downarrow} + N^{\uparrow\uparrow} - BG}\frac{R_{\rm C}P_{\rm S}}{P_{\rm b}P_{\rm t}},$$

where $\frac{N^{\uparrow\downarrow}-N^{\uparrow\uparrow}}{N^{\uparrow\downarrow}-N^{\uparrow\uparrow}}$ is the raw count asymmetry, BG is the background, $P_{\rm b}$ and $P_{\rm t}$ are the beam and target polarizations, $R_{\rm C}$ are the radiative corrections and $P_{\rm S}$ is the pair symmetric background.

The virtual-photon asymmetries A_1 and A_2 are related to the measured asymmetries $A_\parallel$ and $A_\perp$ through

$$A_\parallel = D(A_1 + \eta A_2), \qquad A_\perp = d(A_2 - \zeta A_1)$$

[a] e-mail: dgc3q@virginia.edu

and

$$g_1(x,Q^2) = \frac{\tau}{1+\tau}\left[A_1(x,Q^2) + \frac{1}{\sqrt{\tau}}A_2(x,Q^2)\right]F_1(x,Q^2),$$

where D, η and ζ are kinematic factors, x is the Bjorken scaling variable, $\tau \equiv \frac{\nu^2}{Q^2}$ and $F_1(x,Q^2)$ is the unpolarized structure function. If A_2 is not measured, it can be separated from A_1 by kinematic subtraction or modelled using data from other kinematic regions.

2.1 eg1a

Experiment eg1a was run with a longitudinally polarized electron beam incident on longitudinally polarized proton or deuteron targets with the scattered electron detected in CLAS. The CLAS detector uses a toroidal magnetic field symmetric about the beam axis together with wire drift chambers for track reconstruction, scintillation counters for time-of-flight measurements and threshold Čerenkov and lead-scintillator electromagnetic calorimeters for particle identification.

2.1.1 Polarized beam

The polarized electrons were derived from a strained gallium arsenide photocathode and accelerated and extracted into Hall B at either 2.6 GeV/c or 4.3 GeV/c. The beam polarization was typically 70% and measured frequently with a Moeller polarimeter. The beam helicity was flipped at 1 Hz in a pseudo-random fashion in order to minimize systematic effects. The beam was rastered over the face of the polarized target cell to provide a uniform irradiation of the target material so that differential effects due to beam heating and radiation damage could be minimized. Unfortunately, there was an obstruction in the beam line which did not allow complete raster coverage. As discussed later, the NMR measurement of the polarization was thus compromised and other means of establishing the target polarization had to be used.

2.1.2 Polarized target

The polarized target was mounted at the center of CLAS and consisted of a 5 T superconducting magnet with a ^{4}He evaporation refrigerator operating close to 1 K. The target material was encapsulated in the form of small granules in a cell 1.5 cm diameter by 1 cm long. The material was either $^{15}NH_3$ or $^{15}ND_3$. Proton polarizations of 50% to 70% and deuteron polarizations of 20–25% were obtained by Dynamic Nuclear Polarization. These were measured through the asymmetry in ep elastic scattering [5].

The kinematic coverage was limited to $0.15 < Q^2 < 2.0\,\mathrm{GeV}^2$ at energies of 2.6 and 4.3 GeV. Figure 1 shows the W spectrum obtained from a $^{15}NH_3$ target as well as as a background measurement obtained from a carbon target. Obviously, a large fraction of electrons are scattered

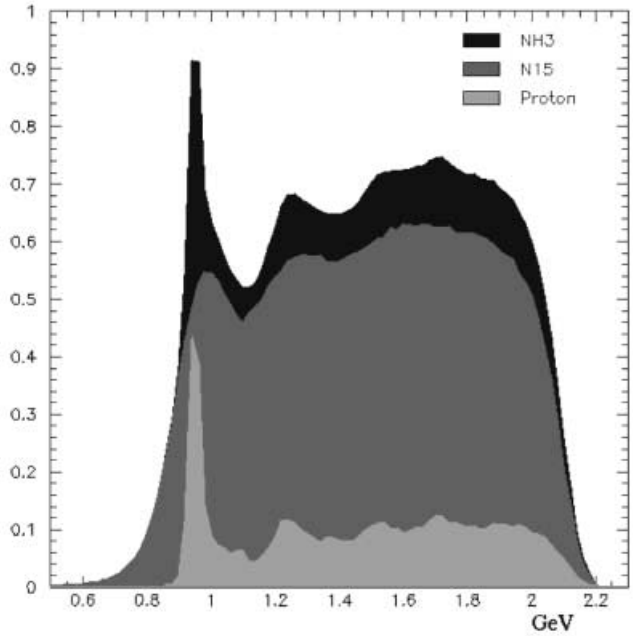

Fig. 1. W spectrum for 4.3 GeV beam energy. The upper curve is for NH_3, the middle curve is the background derived from carbon and empty-target measurements and the lower curve is the difference, attributed to scattering from the free protons in NH_3.

by the nitrogen in the ammonia and from the surrounding helium and target windows. It was not possible for this experiment to measure the background from ^{15}N and so measurements from ^{12}C were made and a target model used to simulate the scattering from ^{15}N.

As described above, the experimental asymmetries $A_\parallel$ were measured and corrected and then used to obtain the combination $A_1 + \eta A_2$ for the proton. Then by using a parameterization of the world data on ep scattering to determine F_1 and a combination of data and a model to calculate A_2 and R, the dominant A_1 and thus g_1 were extracted from the measurement of $A_1 + \eta A_2$. Preliminary results for g_1 *vs.* x at several values of Q^2 are shown in fig. 2.

The solid line shows the results of a calculation using the parameterization described above.

The g_1 were then integrated to obtain the contribution of the data (excluding elastic scattering) to the integral Γ_1^p. This was done by integrating up to the maximum value of W measured at each Q^2. The results are shown as closed squares in fig. 3. The complete integral was obtained by extending to $x = 0$, using the parameterization outlined above (and shown in fig. 2). The complete integral values are shown as open squares in fig. 3, together with data from HERMES and SLAC.

The slope at $Q^2 = 0$ required by the GDH sum rule and the low-Q^2 behaviour predicted by the chiral perturbation calculation of Ji and Osborne [4] are also shown. The curve obtained from the calculations of Burkert and Ioffe [6] is shown and has reasonable agreement with the data, while the calculations of Soffer and Teryaev [7] are

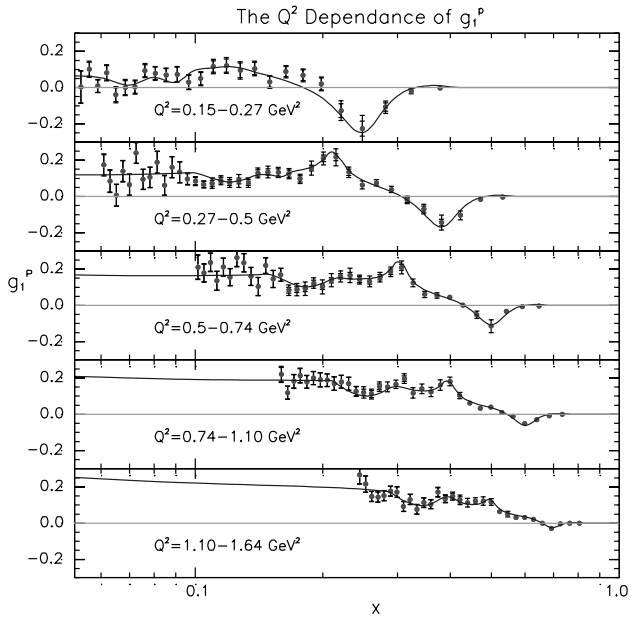

Fig. 2. $g_1(x)$ for the proton, for five Q^2 bins. The solid line is a calculation using a parameterization which combines world data and a model. The data are preliminary.

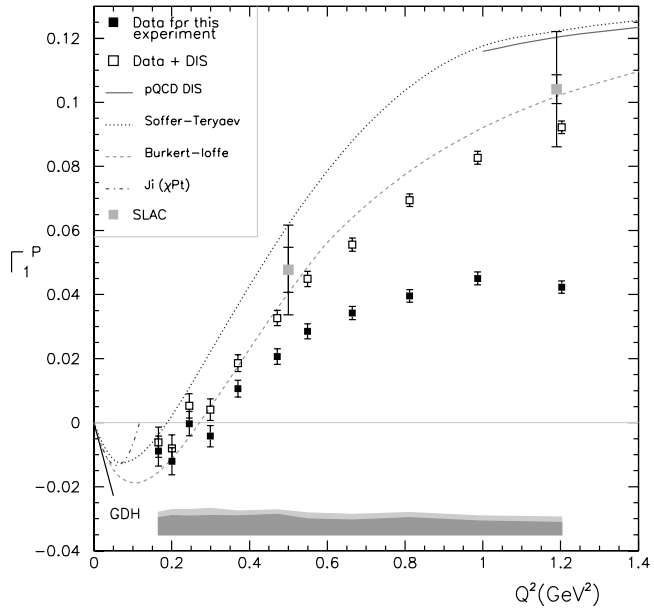

Fig. 3. Preliminary data for Γ_1 *vs.* Q^2 for the proton. The closed squares are from integrating the eg1a data. The open squares include the extension of the integral to $x = 0$. Data from other experiments and several model calculations are included.

in agreement with the data only at low Q^2. The evolution of DIS results to low Q^2, using higher-twist calculations of pQCD [8] is shown as a line at high Q^2. Below $Q^2 \leq 1\,\mathrm{GeV}^2$ Γ_1^p changes rapidly and crosses zero at about $Q^2 = 0.25\,\mathrm{GeV}^2$ for the expected change in sign indicating the dominance of contributions from the resonance region and agreement with the calculation of ref. [6], which ex-

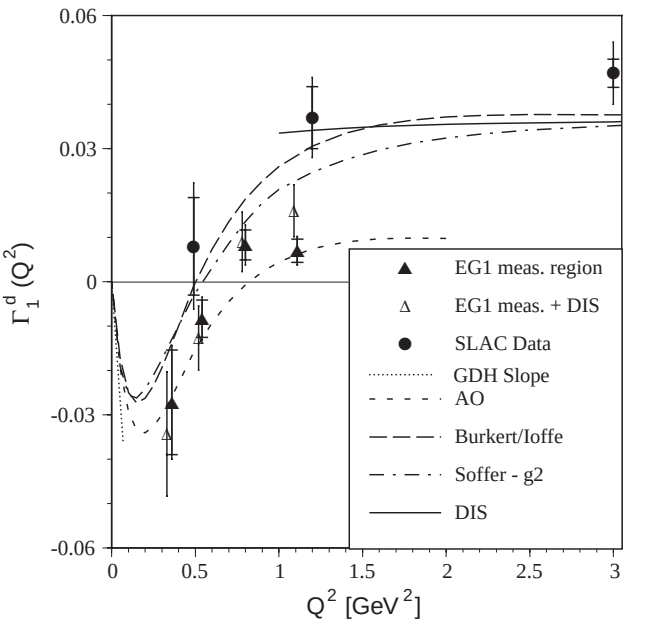

Fig. 4. Γ_1 for the deuteron. The closed triangles are for the integral over the data only. The open triangles include the extension of the integral to $x = 0$. Other data and several model calculations are also included.

plicitly includes s-channel baryon resonances. At the same time there is significant disagreement with the pQCD calculation at higher Q^2.

Figure 4 shows Γ_1 for the deuteron plotted against Q^2. It has the same features as for the proton in fig. 3 though the statistical error is considerably worse. Also the cross-over point is at $Q^2 \approx 0.5$ GeV^2 rather than 0.25 GeV^2.

2.2 eg1b

Experiment eg1b was run from July 2000 to March 2001 and was an improved version of eg1a. Improvements and modifications were made to the polarized target and for the first time a solid ^{15}N target was used for background measurements. Much more data were taken, particularly on the deuteron target, over a wider kinematic range than for eg1a. A total of > 20 billion triggers were accumulated at beam energies of 1.6, 2.5, 4.2 and around 5.7 GeV with a range of $0.05 < Q^2 < 4.5\,\mathrm{GeV}^2$ and $0.8 < W < 3.0$ GeV.

The raw asymmetry at a beam energy of 5.6 GeV and averaged over Q^2 is shown in fig. 5 for both proton and deuteron targets. Structure from several nucleon resonances are seen. Analysis is continuing and there are ten times more events for NH_3 yet to be analysed at 5.7 GeV, allowing the resonance structure to become clearer.

2.3 Resonances Spin Structure (RSS)

The RSS experiment was carried out in Hall C in early 2002. It came immediately after the G_{eN} experiment and used the same apparatus. The polarized target [9] was

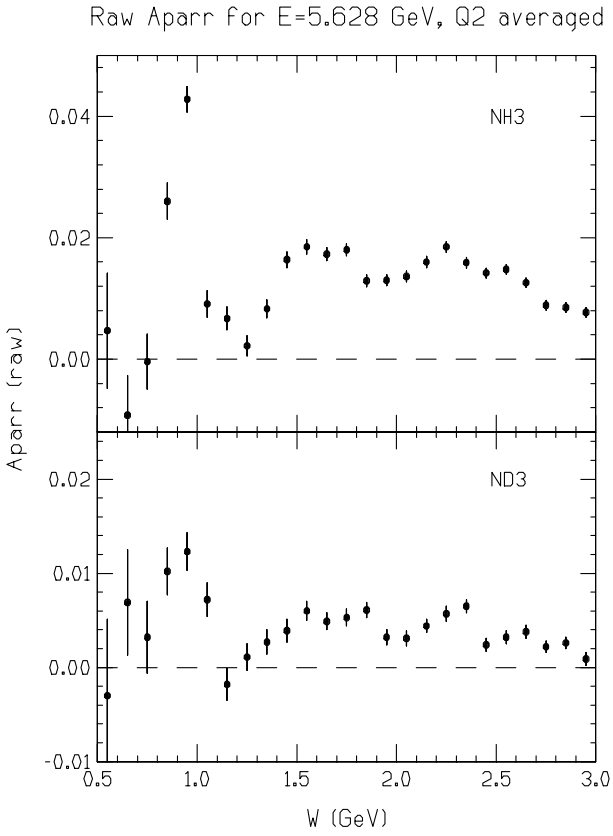

Fig. 5. Raw asymmetries $A_{\parallel}$ *vs.* W for the deuteron, averaged over Q^2 and at a beam energy of 5.628 GeV.

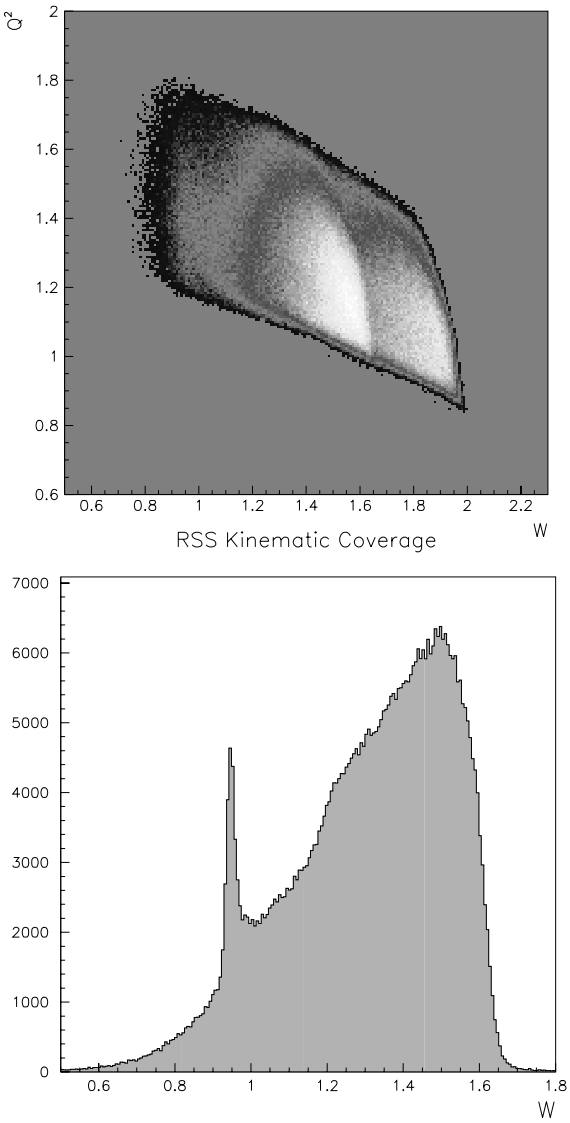

Fig. 6. The kinematic coverage for the RSS experiment and an example of a W spectrum showing a well-defined proton peak.

also the same that had been used previously at SLAC. The experiment measured the proton and deuteron spin asymmetries $A_{\parallel}(x, Q^2)$ and $A_{\perp}(x, Q^2)$ at $Q^2 \approx 1.3$ GeV^2 and $0.8 \leq W \leq 2$ GeV at a beam energy of 5.8 GeV^2. Unlike the eg1 experiments, $A_{\perp}$ was measured directly and will be used in the extraction of Γ_1. Figure 6 shows the acceptance and a raw proton spectrum, giving an idea of the data quality.

2.4 Conclusions

Three experiments at JLab have measured the double polarization asymmetry, $A_{\parallel}(x, Q^2)$ in the resonance region. From these measurements the spin structure function can be extracted and integrated to obtain the first moment $\Gamma_1 = \int g_1(x, Q^2)\mathrm{d}x$.

The analysis from the first experiment, eg1a, is nearly finished and Γ_1 shows a rapidly changing behaviour at low Q^2, crossing zero at $Q^2 \approx 0.25$ GeV^2 for the proton and $Q^2 \approx 0.5$ GeV^2 for the deuteron. This is in reasonable agreement with the model of Burkert and Ioffe [6]. At the highest Q^2 for this experiment the data are in disagreement with a pQCD evolution down from the DIS region.

Experiment eg1b covered a much bigger kinematic range than eg1a with much greater precision. Some asymmetries are being generated but, as yet, no data for Γ_1 are available.

Experiment RSS measured $A_{\parallel}(x, Q^2)$ at $Q^2 \approx 1.3\,\mathrm{GeV}^2$ and over a range of W. Of the three experiments it was the only one to measure $A_{\perp}(x, Q^2)$ explicitly. Analysis is continuing.

So, in the near future we can look forward to much more data, which will allow for the extraction of Γ_1 for the neutron.

References

1. S. Gerasimov, Yad. Fiz. **2**, 598 (1965); S.D. Drell, A.C. Hearn, Phys. Rev. Lett. **16**, 908 (1966).
2. J. Ahrens *et al.*, hep-ex/0105089 (2001).
3. G. Anton, Few-Body Syst. Suppl. **11**, 177 (1999).
4. X. Ji, G. Osborne, J. Phys. G **27**, 127 (2001).
5. C. Keith *et al.*, submitted to Nucl. Instrum. Methods.

6. V. Burkert, B. Ioffe, Phys. Lett. B **296**, 223 (1992); J. Exp. Theor. Phys. **78**, 619 (1994).
7. J. Soffer, O. Teryaev, Phys. Rev. Lett. **70**, 3372 (1993); Phys. Rev. D **51**, 25 (1995).
8. S.A. Larin, J.A.M. Vermaseren, Phys. Lett. B **259**, 345 (1991).
9. D.G. Crabb, D. Day *et al.*, Nucl. Instrum. Methods A **356**, 9 (1995).